

Article

Dynamics of Optimal Cue Integration with Time-Varying Delay in the Insects' Navigation System

Molan Li *, Da Li, Junxing Zhang, Xuanlu Xiang and Di Zhao

School of Mathematics and Information Science, Guangxi University, Nanning 530004, China

* Correspondence: moonlanlee@163.com

Abstract: Neural networks with a ring structure are considered biologically plausible and have the ability of enforcing unique and persistent heading representations, yielding realistic homing behaviors. Recent studies have found that insects optimally integrate sensory information from the environment for head direction by using ring attractor networks. Optimal cue integration as the basic component of a complex insect navigation system proves to consist of a ring attractor network that is coupled by some integration neurons and some uniform inhibition neurons. The dynamics of the coupled mechanisms between neurons in optimal cue integration determine whether the insects' homing capability is affected by environmental noises. Furthermore, time delays caused by communication between different kinds of neurons may induce complex dynamical properties. These dynamical behaviors are essential for understanding the neural mechanisms of insect homing behaviors, but there is a lack of relevant research on the dynamics of optimal cue integration with time-varying delay in the insects' navigation system. In this paper, we discuss the dynamical properties of optimal cue integration with time-varying delay and show that it is asymptotically stable and leads to a unique insect home direction. These results are critical in providing the theoretical basis for further research on insect homing behaviors and the establishment of autonomous robots that mimic insect navigation mechanisms in the future.

Keywords: neural network; time-varying delay; stability; Lyapunov–Krasovskii functional; linear matrix inequality

MSC: 92B20; 34D05



Citation: Li, M.; Li, D.; Zhang, J.; Xiang, X.; Zhao, D. Dynamics of Optimal Cue Integration with Time-Varying Delay in the Insects' Navigation System. *Mathematics* **2023**, *11*, 3696. <https://doi.org/10.3390/math11173696>

Academic Editor: Benjamin Ambrosio

Received: 13 August 2023

Revised: 24 August 2023

Accepted: 26 August 2023

Published: 28 August 2023



Copyright: © 2023 by the authors. Licensee MDPI, Basel, Switzerland. This article is an open access article distributed under the terms and conditions of the Creative Commons Attribution (CC BY) license (<https://creativecommons.org/licenses/by/4.0/>).

1. Introduction

In recent studies, the CX (central complex) of the insect midbrain has been shown to act as a navigational center in insect navigation, and CX-based mechanisms flexibly coordinate guidance strategies across sensory domains using biologically plausible ring attractor networks [1,2]. A ring attractor network mathematically describes the dynamical behaviors of neural circuits, and its properties of local excitation and long-range inhibition are ubiquitous across many brain areas and across many animal taxa [3–8]. As a canonical model for neural information representation, the ring attractor network constructs an appropriate map between the external states in the world and the attractor states in the insect brain [9,10] and demonstrates its efficiency in explaining the neural mechanisms responsible for orientation representation, such as modeling motor responses to external stimuli, tracking anticipation, and integrating multisensory cues [11,12].

Cue integration is common in insect navigation [13,14]. Despite facing external factors like wind gusts or similar odors, insects still aim for the nest and consistently use a sophisticated integration strategy that yields applicable navigational behaviors across contexts [15,16]. Such insect-inspired artificial intelligence (AI) optimizes the resource efficiency and computing capabilities of small, autonomous mobile robots [17].

Heading direction for insects is related to the activity of neurons in the CX [18,19]. As the primary basis in the insects' navigation system, optimal cue integration is presented as

consisting of two kinds of neurons (integration neurons and uniform inhibition neurons), which are coupled as a ring attractor network [20]. Additionally, noises may lead to representational “drift”, indicating that neural population codes in many brain areas continuously change even when animals have fully learned and stably performed their tasks [21]. However, the dynamics of neurons in the ring attractor network robustly resist random drifts and distractions and drive the perturbation to stability [9]. The light cue experiments in rats suggest that when rats navigate until they reach a specific location, the firing rate of neurons in the CX will approach a fixed value [22]. The interaction of attractor dynamics and neuromodulation allows the insects’ motor commands to align with the current target [23].

Research on neural networks with a ring structure mainly focuses on the discussion of their neural basis and computational properties. Vafidis et al. proposed a synaptic plasticity rule in an attractor network that maintains the connectivity required for path integration [24]. Kutschireiter et al. proposed a Bayesian ring attractor to implement near-optimal angular path integration and evidence accumulation [25]. Yu et al. investigated the type and shape of the attractors in a ring attractor network based on specific conditions [26]. A rigorous analysis of the dynamical properties of a ring attractor network with two kinds of neurons coupled is currently lacking, and studies on these dynamical behaviors are rarely correlated to insect homing behaviors in the real environment.

Insects are able to convert spatiotemporal changes into orientation signals [27]. Since optimal cue integration proposed in existing studies is relatively simple [15,16] and time delays are one of the main features of information transmission between neurons in insect brains, optimal cue integration with time-varying delay is able to greatly emulate biological neural networks in detail. Time delay is a hot topic in the study of neural networks [28–31]. The presence of time delay may lead to oscillations and instabilities, which deteriorate the performance of neural networks [32–34].

Numerous studies on the stability of a wide range of neural networks with time delays are based on linear matrix inequalities (LMIs). Guo et al. discussed the sufficient conditions for asymptotic stability of delayed memristive neural networks [35]. Zheng et al. investigated the stability on delayed T-S fuzzy state feedback controller of the singular uncertain system [36]. Maharajan et al. handled the problem of globally exponential stability analysis in impulsive Cohen–Grossberg BAM neural networks with time delays [37]. Chen et al. studied the conditions for exponential stability in nonlinear time-delay systems under flexible delayed impulsive control [38]. But these are all based on traditional neural networks, with few achievements in neural networks with a ring structure.

Thus, inspired by the aforementioned analysis and based on Lyapunov–Krasovskii functionals, some inequality techniques, and LMIs, the paper focuses on the dynamics of optimal cue integration with time-varying delay and coupled properties. The major contributions are summarized as follows:

- We introduce a time delay into the mechanisms of optimal cue integration to emulate biological neural networks in insect brains. The improved system for optimal cue integration becomes more complex and has better compatibility than the one proposed before [16,20].
- We study the dynamical properties of the system for optimal cue integration, which is a neural network with a ring structure. We obtain conditions for the existence and uniqueness of the equilibrium point in the system by employing the uniqueness theorem [39]. Taking the size of the time delay into account, we also obtain some delay-dependent asymptotic stability conditions for this system, which are more in line with the real situation of delayed information transmission in insect brains, based on Lyapunov–Krasovskii functionals [40].
- By linking the experimental observations with mathematical properties from a dynamic point of view, we shed light on the fact that optimal cue integration in the insects’ navigation system plays a crucial role in directly driving insects back to their target location, their nest, without being affected by complex environmental changes.

The outline of the paper is arranged as follows. Section 2 presents the improved system for optimal cue integration with coupled property and time-varying delay, as well as some illustrations of the system. Section 3 presents the dynamical properties of the system of optimal cue integration and some conditions under which insects are able to optimally integrate the noisy information available to them and return to the nest. Section 4 presents some numerical examples to illustrate the validity of the main results.

Notations: \mathbb{R} denotes the set of real numbers. \mathbb{R}^n and $\mathbb{R}^{m \times n}$ denote the n -dimensional Euclidean space and the set of all $m \times n$ real matrices, respectively. For a real matrix A , $A > 0$ ($A < 0$) indicates that A is symmetric and positive definite (negative definite), whereas $A \geq 0$ ($A \leq 0$) represents a positive (negative) semidefinite matrix. Matrices are assumed to have compatible dimensions if not explicitly stated.

2. Problem Formulation

The system for optimal cue integration with time-varying delay in the insects' navigation system is as follows:

$$\tau \dot{C}_{IN} = -C_{IN} + \sum_{j=1}^s W_{E2E}^{ji} g(C_{IN}^j) + W_{I2E} g(C_{UI}(t - d(t))) + c_i, \quad i = 1, \dots, s, \tag{1}$$

$$\tau \dot{C}_{UI} = -C_{UI} + W_{I2I} g(C_{UI}) + W_{E2I} \sum_{k=1}^p g(C_{IN}^k(t - d(t))), \quad k = 1, \dots, p, \tag{2}$$

where C_{IN} and C_{UI} represent the firing rates of integration neurons (IN) and uniform inhibition neurons (UI), respectively. Integration neurons have recurrent excitatory connections to each other in a ring attractor network to optimally integrate different cues from the input, so $W_{E2E} = (W_{E2E}^{ji})_{s \times s}$ is the matrix of connected weights between integration neuron j and integration neuron i . Uniform inhibition neurons also have the same positive feedback to each other in this ring because of the interaction between neurons of the same functional type, so $W_{I2I} = (W_{I2I}^{km})_{p \times p}$, $m = 1, 2, \dots, p$ is the connected weight matrix between uniform inhibition neurons. Obviously, the matrices W_{E2E} and W_{I2I} are symmetric because the neurons in each matrix are of the same kind.

In addition, uniform inhibition neurons sum up activations from all integration neurons, and the coupled mechanisms between neurons for optimal integration require consideration of time delays due to the information transmission occurring in neurons, such that $W_{E2I} = (W_{E2I}^{mi})_{p \times s}$ represents the delayed connection weight matrix from integration neuron m to uniform inhibition neuron i . The uniform inhibition neurons also inhibit all integration neurons, such that $W_{I2E} = (W_{I2E}^{im})_{s \times p}$ is the delayed connection weight matrix from uniform inhibition neurons to integration neurons. The inhibitory effect of uniform inhibition neurons on integration neurons results in negative connection weights, i.e., $(W_{I2E}^{im})_{s \times p} < 0$. The activation function is $g(x)$ with $g(0) = 0$, wherein *tanh*, *sigmoid*, and *ReLU* are typical examples. c_i represents the input cue constant. Note that $C_{UI}(t - d(t))$ and $C_{IN}^k(t - d(t))$ are interaction terms, and $d(t)$ describes the time delay between uniform inhibition neurons and integration neurons in signal transmission. For the sake of simplicity, let the positive time constant τ be 1.

As a result of the above discussion, the system for optimal cue integration can be formulated in the following form:

$$\begin{aligned} [\dot{C}_{IN}^1, \dots, \dot{C}_{IN}^s, \dot{C}_{UI}^1, \dots, \dot{C}_{UI}^p]^T &= -[C_{IN}^1, \dots, C_{IN}^s, C_{UI}^1, \dots, C_{UI}^p]^T + \begin{bmatrix} (W_{E2E})_{s \times s} & 0 \\ 0 & (W_{I2I})_{p \times p} \end{bmatrix}_{n \times n} \\ &\times [g_1(C_{IN}^1), \dots, g_s(C_{IN}^s), g_{s+1}(C_{UI}^1), \dots, g_n(C_{UI}^p)]^T + \begin{bmatrix} 0 & (W_{I2E})_{s \times p} \\ (W_{E2I})_{p \times s} & 0 \end{bmatrix}_{n \times n} \\ &\times [g_1(C_{IN}^1(t - d(t))), \dots, g_s(C_{IN}^s(t - d(t))), g_{s+1}(C_{UI}^1(t - d(t))), \dots, g_n(C_{UI}^p(t - d(t)))]^T \\ &+ [c_1, \dots, c_s, 0, \dots, 0]^T, \quad s + p = n. \end{aligned} \tag{3}$$

The activation functions $g_i(\cdot)$ satisfy the following inequalities with $g_i(0) = 0$:

$$0 \leq \frac{g_i(\tilde{c}_1) - g_i(\tilde{c}_2)}{\tilde{c}_1 - \tilde{c}_2} \leq k_i, \quad i = 1, 2, \dots, n, \quad \forall \tilde{c}_1 \neq \tilde{c}_2, \tag{4}$$

where $k_i (i = 1, 2, \dots, n)$ are constants that are not negative and we let $K = \text{diag}(k_1, k_2, \dots, k_n)$. \tilde{c}_1 and \tilde{c}_2 are arbitrary constants and the functions $g_i(\cdot), i = 1, 2, \dots, n$ are Lipschitz continuous. For simplicity, let $g(\cdot)$ be \tanh .

In addition, $d(t)$ denotes the time-varying bounded state delay satisfying

$$0 \leq d(t) \leq \bar{d}, \quad \dot{d}(t) \leq h, \tag{5}$$

where \bar{d} and h are positive scalars.

The initial conditions associated with (3) are given as follows:

$$[C_{IN}^1, \dots, C_{IN}^s, C_{UI}^1, \dots, C_{UI}^p]^T = \phi(y), \quad y \in [-\bar{d}, 0], \tag{6}$$

where $\phi(y)$ is a continuous function vector.

3. Existence and Stability of the Stationary Solution to the System for Optimal Cue Integration

In this section, we discuss the dynamical properties of the system for optimal cue integration and decide to begin by proving this system (3) has an invariant set. We assume $C^* = (C_1^*, C_2^*, \dots, C_n^*)^T$ is an equilibrium of system (3). By the coordinate transformation $x(\cdot) = [x_1(t), \dots, x_n(t)]^T = [C_{IN}^1, \dots, C_{IN}^s, C_{UI}^1, \dots, C_{UI}^p]^T - C^*$, we obtain the following system:

$$\dot{x}(t) = -x(t) + \begin{bmatrix} (W_{E2E})_{s \times s} & 0 \\ 0 & (W_{I2I})_{p \times p} \end{bmatrix} f(x(t)) + \begin{bmatrix} 0 & (W_{I2E})_{s \times p} \\ (W_{E2I})_{p \times s} & 0 \end{bmatrix} f(x(t - d(t))), \tag{7}$$

$f(x(t)) = [f_1(x_1(t)), f_2(x_2(t)), \dots, f_n(x_n(t))]^T$, in which $f_i(x_i(t)) = g_i(x_i(t) + C_i^*) - g_i(C_i^*)$. We set

$$W_0 = (w_{ij}^0)_{n \times n} = \begin{bmatrix} W_{E2E} & 0 \\ 0 & W_{I2I} \end{bmatrix}_{n \times n}, \quad \tilde{W} = (\tilde{w}_{ij})_{n \times n} = \begin{bmatrix} 0 & W_{I2E} \\ W_{E2I} & 0 \end{bmatrix}_{n \times n}.$$

Proposition 1. System (7) has an invariant set

$$P = \{x \mid |x_j| \leq 4, (j = 1, \dots, n)\}. \tag{8}$$

Proof of Proposition 1. For each $x(0) \in P$, we have

$$x_j(t) = x_j(0)e^{-t} + \int_0^t e^{-(t-r)} (W_0 f(x(t)) + \tilde{W} f(x(t - d(t)))) dr. \tag{9}$$

From [16,20], the absolute value of the weights of recurrent connections between each neuron in the system is equal to or less than 1, so that $0 \leq w_{ij}^0 \leq 1$ and $-1 \leq \tilde{w}_{ij} \leq 0$, $(i, j = 1, \dots, n)$. According to $f_i(x_i(t)) = g_i(x_i(t) + C^*) - g_i(C^*)$ and $g(\cdot) = \tanh(\cdot)$, we obtain $-2 \leq f_i(\cdot) \leq 2$. Then, from the above analysis and equality (9), there is

$$\begin{aligned} |x_j(t)| &\leq |x_j(0)|e^{-t} + \int_0^t e^{-(t-r)} |(W_0 f(x(t)) + \tilde{W} f(x(t - d(t))))| dr \\ &\leq 4e^{-t} + \int_0^t 4e^{-(t-r)} dr \\ &= 4, \quad t \geq 0. \end{aligned} \tag{10}$$

So $x(t) \in P$. The proof is complete. \square

In Proposition 1, we show that system (7) has an invariant set. This suggests that the firing rates of neurons in the system of optimal cue integration stay within a range. Then, we will give the existence and uniqueness conditions of the stationary solution to system (7) in this invariant set.

Proposition 2. Under condition (4), the stationary solution $x = 0$ to system (7) is unique if there exist positive definite diagonal matrices $R \in \mathbb{R}^{n \times n}$, $V \in \mathbb{R}^{n \times n}$ and real constants $\gamma > 0$, $0 < q \leq 1$ such that the following LMI holds:

$$\Phi = \begin{bmatrix} 2RK^{-1} - RW_0 - W_0^T R - q^{-1}\gamma V & * \\ -\frac{1}{\sqrt{q}}R\tilde{W} & q^{-1}\gamma V \end{bmatrix} > 0, \tag{11}$$

where $*$ represents the transpose of the corresponding matrix.

Proof of Proposition 2. The equilibrium point x^* of system (7) is given by

$$-x^* + W_0f(x^*) + \tilde{W}f(x^*) = 0. \tag{12}$$

Equation (12) indicates that if $f(x^*) = 0$, then $x^* = 0$. Suppose that $f(x^*) \neq 0$, multiplying both sides of Equation (12) by $2f^T(x^*)R \neq 0$, and then plus and minus $q^{-1}\gamma f^T(x^*)Vf(x^*) - q^{-1}$ yields

$$\begin{aligned} & -2f^T(x^*)Rx^* + 2f^T(x^*)RW_0f(x^*) + 2f^T(x^*)R\tilde{W}f(x^*) \\ & + q^{-1}\gamma f^T(x^*)Vf(x^*) - q^{-1}\gamma f^T(x^*)Vf(x^*) = 0. \end{aligned} \tag{13}$$

Since $0 < q \leq 1$, there is

$$\begin{aligned} & -2f^T(x^*)Rx^* + 2f^T(x^*)RW_0f(x^*) + 2f^T(x^*)R\tilde{W}f(x^*) \\ & + q^{-1}\gamma f^T(x^*)Vf(x^*) - \gamma f^T(x^*)Vf(x^*) \geq 0. \end{aligned} \tag{14}$$

Note that inequality (4) given before can be used to acquire

$$f_i^2(x_i(\cdot)) \leq k_i x_i(\cdot) f_i(x_i(\cdot)) \leq k_i^2 x_i^2(\cdot). \tag{15}$$

From inequalities (15), we have

$$-\sum_{i=1}^n k_i x_i^* f_i(x_i^*) \leq -\sum_{i=1}^n f_i^2(x_i^*). \tag{16}$$

Thus,

$$-2f^T(x^*)Rx^* \leq -2f^T(x^*)RK^{-1}f(x^*). \tag{17}$$

According to Lemma 2.3 presented by [39], the following inequality holds:

$$-\gamma f^T(x^*)Vf(x^*) + 2f^T(x^*)R\tilde{W}f(x^*) \leq \gamma^{-1}f^T(x^*)\tilde{W}^T RV^{-1}R\tilde{W}f(x^*). \tag{18}$$

Then, we combine (14), (17), and (18), for any $f(x^*) \neq 0$, yielding

$$\begin{aligned} & 2f^T(x^*)RW_0f(x^*) - 2f^T(x^*)RK^{-1}f(x^*) + q^{-1}\gamma f^T(x^*)Vf(x^*) \\ & + \gamma^{-1}f^T(x^*)\tilde{W}^T RV^{-1}R\tilde{W}f(x^*) \geq 0, \end{aligned} \tag{19}$$

and it can be rewritten as

$$f^T(x^*)(-2RK^{-1} + RW_0 + W_0^T R + \gamma^{-1}\tilde{W}^T RV^{-1}R\tilde{W} + q^{-1}\gamma V)f(x^*) \geq 0. \tag{20}$$

However, by Schur complement theory and condition (11), it follows that

$$f^T(x^*)(-2RK^{-1} + RW_0 + W_0^T R + \gamma^{-1}\tilde{W}^T R V^{-1} R \tilde{W} + q^{-1}\gamma V)f(x^*) < 0. \tag{21}$$

□

The conflict in (20) and (21) implies that the assumption $f(x^*) \neq 0$ fails. That is, with condition (11), the solution $x = 0$ is the unique solution, i.e., the unique stationary solution to system (7). This indicates that the unique equilibrium point may correspond to their unique target (nest) for insects. Based on the existence and uniqueness of the stationary solution to this system, we next discuss its stability under the time delay derivative $h < 1$ to demonstrate that foraging insects are able to robustly integrate their route from environmental disturbances, aim for the nest, and return to it under communication delays between different kinds of neurons.

Proposition 3. *If $h < 1$ and there exist a symmetric positive definite matrix $P \in \mathbb{R}^{n \times n}$, positive definite matrices $F_1 \in \mathbb{R}^{n \times n}$, $F_2 \in \mathbb{R}^{n \times n}$ and positive diagonal matrices $N_1 \in \mathbb{R}^{n \times n}$, $N_2 \in \mathbb{R}^{n \times n}$ such that the following LMI holds:*

$$\Gamma = \begin{bmatrix} \eta_{11} & 0 & \eta_{13} & \eta_{14} \\ * & \eta_{22} & 0 & \eta_{24} \\ * & * & \eta_{33} & \eta_{34} \\ * & * & * & \eta_{44} \end{bmatrix} < 0, \tag{22}$$

where

$$\begin{aligned} \eta_{11} &= -PI - IP + F_1, \\ \eta_{13} &= PW_0 + KN_1 - E^T, \\ \eta_{14} &= P\tilde{W}, \\ \eta_{22} &= -(1 - h)F_1, \\ \eta_{24} &= KN_2, \\ \eta_{33} &= -2N_1 + EW_0 + W_0^T E^T + F_2, \\ \eta_{34} &= E\tilde{W}, \\ \eta_{44} &= -2N_2 - (1 - h)F_2, \end{aligned}$$

then, the stationary solution $x = 0$ to system (7) is asymptotically stable.

Proof of Proposition 3. We construct the following Lyapunov–Krasovskii function candidates:

$$V(t, x(t)) = V_1(t, x(t)) + V_2(t, x(t)) + V_3(t, x(t)), \tag{23}$$

where

$$\begin{aligned} V_1(t, x(t)) &= x^T(t)Px(t), \\ V_2(t, x(t)) &= 2 \sum_{i=1}^n e_i \int_0^{x_i(t)} f_i(y)dy, \\ V_3(t, x(t)) &= \int_{t-d(t)}^t x^T(y)F_1x(y)dy + \int_{t-d(t)}^t f^T(x(y))F_2f(x(y))dy, \end{aligned}$$

and $e_i (i = 1, \dots, n)$ are positive scalars. The time derivative of $V_i(t, x(t))$ along system (7) is separately given as follows:

$$\begin{aligned} \dot{V}_1(t, x(t)) &= 2x^T(t)P\dot{x}(t) \\ &= 2x^T(t)P\left(-x(t) + W_0f(x(t)) + \tilde{W}f(x(t-d(t)))\right), \end{aligned} \tag{24}$$

$$\begin{aligned} \dot{V}_2(t, x(t)) &= 2 \sum_{i=1}^n e_i f_i(x_i(t))\dot{x}(t) \\ &= 2f^T(x(t))E\left(-x(t) + W_0f(x(t)) + \tilde{W}f(x(t-d(t)))\right), \end{aligned} \tag{25}$$

$$\begin{aligned} \dot{V}_3(t, x(t)) &\leq x^T(t)F_1x(t) - (1-h)x^T(t-d(t))F_1x(t-d(t)) \\ &\quad + f^T(x(t))F_2f(x(t)) - (1-h)f^T(x(t-d(t)))F_2f(x(t-d(t))), \end{aligned} \tag{26}$$

where $E = \text{diag}(e_i)$. Moreover, under inequality (15), there are two positive diagonal matrices N_1 and N_2 such that

$$\begin{aligned} x^T(t)KN_1f(x(t)) - f^T(x(t))N_1f(x(t)) &\geq 0, \\ x^T(t-d(t))KN_2f(x(t-d(t))) - f^T(x(t-d(t)))N_2f(x(t-d(t))) &\geq 0. \end{aligned} \tag{27}$$

Then, we have

$$\begin{aligned} \dot{V}(t, x(t)) &= \dot{V}_1(t, x(t)) + \dot{V}_2(t, x(t)) + \dot{V}_3(t, x(t)) \\ &\leq 2x^T(t)P\left(-x(t) + W_0f(x(t)) + \tilde{W}f(x(t-d(t)))\right) \\ &\quad + 2f^T(x(t))E\left(-x(t) + W_0f(x(t)) + \tilde{W}f(x(t-d(t)))\right) \\ &\quad + x^T(t)F_1x(t) - (1-h)x^T(t-d(t))F_1x(t-d(t)) \\ &\quad + f^T(x(t))F_2f(x(t)) - (1-h)f^T(x(t-d(t)))F_2f(x(t-d(t))) \\ &\quad + 2[x^T(t)KN_1f(x(t)) - f^T(x(t))N_1f(x(t))] \\ &\quad + 2[x^T(t-d(t))KN_2f(x(t-d(t))) - f^T(x(t-d(t)))N_2f(x(t-d(t)))] \\ &= [x^T(t), x^T(t-d(t)), f^T(x(t)), f^T(x(t-d(t)))]\Gamma \begin{bmatrix} x(t) \\ x(t-d(t)) \\ f(x(t)) \\ f(x(t-d(t))) \end{bmatrix}. \end{aligned} \tag{28}$$

□

According to condition (22), we obtain $\dot{V}(t, x(t)) \leq 0$ ($V = 0$ only if $x = 0$). This indicates that system (7) is asymptotically stable.

Many studies have proposed two criteria for stability in delayed systems [41–45]. One is the delay-independent criteria, under which the system only remains stable if the condition is satisfied at all times. We have already derived such a delay-independent criterion through the above analysis. The other is the delay-dependent criteria, which, in contrast to the delay-independent criteria, tend to be accurate since the delay function is included as a parameter in the stability criteria. This kind of criterion with finite time delays is more suitable for neural networks with time delays caused by actual signal transmission. For this problem, when $h < 1$, we will discuss the delay-dependent asymptotic stability of system (7).

Proposition 4. *If $h < 1$ and there exist a symmetric positive definite matrix $P \in \mathbb{R}^{n \times n}$, positive definite matrices $F_1 \in \mathbb{R}^{n \times n}$, $F_2 \in \mathbb{R}^{n \times n}$ and positive diagonal matrices $N_1 \in \mathbb{R}^{n \times n}$, $N_2 \in \mathbb{R}^{n \times n}$ such that the following LMIs hold:*

$$X = \begin{bmatrix} X_{11} & X_{12} & X_{13} & X_{14} & X_{15} \\ * & X_{22} & X_{23} & X_{24} & X_{25} \\ * & * & X_{33} & X_{34} & X_{35} \\ * & * & * & X_{44} & X_{45} \\ * & * & * & * & X_{55} \end{bmatrix} \geq 0 \tag{29}$$

$$\Gamma = \begin{bmatrix} \eta_{11} & \eta_{12} & \eta_{13} & \eta_{14} \\ * & \eta_{22} & \eta_{23} & \eta_{24} \\ * & * & \eta_{33} & \eta_{34} \\ * & * & * & \eta_{44} \end{bmatrix} < 0, \tag{30}$$

where

$$\begin{aligned} \eta_{11} &= -PI - IP + X_{15}^T + X_{15} + F_1 + \bar{d}X_{55} + \bar{d}X_{11}, \\ \eta_{12} &= X_{25}^T - X_{15} + \bar{d}X_{12}, \\ \eta_{13} &= PW_0 + X_{35}^T + KN_1 - E^T - \bar{d}X_{55}W_0 + \bar{d}X_{13}, \\ \eta_{14} &= P\tilde{W} + X_{45}^T - \bar{d}X_{55}\tilde{W} + \bar{d}X_{14}, \\ \eta_{22} &= -X_{25}^T - X_{25} + \bar{d}X_{22} - (1 - h)F_1, \\ \eta_{23} &= -X_{35}^T + \bar{d}X_{23}, \\ \eta_{24} &= -X_{45}^T + KN_2 + \bar{d}X_{24}, \\ \eta_{33} &= -2N_1 + EW_0 + W_0^T E^T + \bar{d}W_0^T X_{55}W_0 + \bar{d}X_{33} + F_2, \\ \eta_{34} &= E\tilde{W} + \bar{d}W_0^T X_{55}\tilde{W} + \bar{d}X_{34}, \\ \eta_{44} &= -2N_2 + \bar{d}\tilde{W}^T X_{55}\tilde{W} + \bar{d}X_{44} - (1 - h)F_2, \end{aligned}$$

then, the stationary solution $x = 0$ to system (7) is asymptotically stable.

Proof of Proposition 4. Considering the following Lyapunov functional candidates:

$$V(t, x(t)) = V_1(t, x(t)) + V_2(t, x(t)) + V_3(t, x(t)) + V_4(t, x(t)) + V_5(t, x(t)), \tag{31}$$

with

$$\begin{aligned} V_1(t, x(t)) &= x^T(t)Px(t), \\ V_2(t, x(t)) &= 2 \sum_{i=1}^n e_i \int_0^{x_i(t)} f_i(y)dy, \\ V_3(t, x(t)) &= \int_0^t \int_{\delta-d(t)}^{\delta} v^T X v dy d\delta, \\ V_4(t, x(t)) &= \int_{t-\bar{d}}^t (\bar{d} + y - t) \dot{x}^T(y) X_{55} \dot{x}(y) dy, \\ V_5(t, x(t)) &= \int_{t-d(t)}^t x^T(y) F_1 x(y) dy + \int_{t-d(t)}^t f^T(x(y)) F_2 f(x(y)) dy, \end{aligned}$$

where $e_i (i = 1, \dots, n)$ are positive scalars and $v = [x^T(\delta), x^T(\delta - d(\delta)), f^T(x(\delta)), f^T(x(\delta - d(\delta))), \dot{x}^T(y)]^T$, we can establish the derivative of $V_i(t, x(t))$ as follows:

$$\begin{aligned} \dot{V}_1(t, x(t)) &= 2x^T(t)P\dot{x}(t) \\ &= 2x^T(t)P\left(-x(t) + W_0f(x(t)) + \tilde{W}f(x(t - d(t)))\right), \end{aligned} \tag{32}$$

$$\begin{aligned} \dot{V}_2(t, x(t)) &= 2 \sum_{i=1}^n e_i f_i(x_i(t)) \dot{x}(t) \\ &= 2f^T(x(t))E\left(-x(t) + W_0f(x(t)) + \tilde{W}f(x(t - d(t)))\right), \end{aligned} \tag{33}$$

$$\dot{V}_3(t, x(t)) \leq \bar{d}[x^T(t), x^T(t - d(t)), f^T(x(t)), f^T(x(t - d(t)))] \tag{34}$$

$$\begin{aligned} & \times \begin{bmatrix} X_{11} & X_{12} & X_{13} & X_{14} \\ * & X_{22} & X_{23} & X_{24} \\ * & * & X_{33} & X_{34} \\ * & * & * & X_{44} \end{bmatrix} \begin{bmatrix} x(t) \\ x(t - d(t)) \\ f(x(t)) \\ f(x(t - d(t))) \end{bmatrix} \\ & + 2[x^T(t), x^T(t - d(t)), f^T(x(t)), f^T(x(t - d(t)))] \begin{bmatrix} X_{15} \\ X_{25} \\ X_{35} \\ X_{45} \end{bmatrix} \\ & \times (x(t) - x(t - d(t))) + \int_{t-\bar{d}}^t \dot{x}^T(y) X_{55} \dot{x}(y) dy, \end{aligned}$$

$$\dot{V}_4(t, x(t)) = \bar{d}\dot{x}^T(t) X_{55} \dot{x}(t) - \int_{t-\bar{d}}^t \dot{x}^T(y) X_{55} \dot{x}(y) dy, \tag{35}$$

$$\begin{aligned} \dot{V}_5(t, x(t)) & \leq x^T(t) F_1 x(t) - (1 - h)x^T(t - d(t)) F_1 x(t - d(t)) \\ & + f^T(x(t)) F_2 f(x(t)) - (1 - h)f^T(x(t - d(t))) F_2 f(x(t - d(t))), \end{aligned} \tag{36}$$

where $E = \text{diag}(e_i)$. Then, we can obtain

$$\begin{aligned} \dot{V}(t, x(t)) & = \dot{V}_1(t, x(t)) + \dot{V}_2(t, x(t)) + \dot{V}_3(t, x(t)) + \dot{V}_4(t, x(t)) + \dot{V}_5(t, x(t)) \\ & \leq 2x^T(t) P \left(-x(t) + W_0 f(x(t)) + \tilde{W} f(x(t - d(t))) \right) \\ & + 2f^T(x(t)) E \left(-x(t) + W_0 f(x(t)) + \tilde{W} f(x(t - d(t))) \right) \\ & + \bar{d}[x^T(t), x^T(t - d(t)), f^T(x(t)), f^T(x(t - d(t)))] \\ & \times \begin{bmatrix} X_{11} & X_{12} & X_{13} & X_{14} \\ * & X_{22} & X_{23} & X_{24} \\ * & * & X_{33} & X_{34} \\ * & * & * & X_{44} \end{bmatrix} \begin{bmatrix} x(t) \\ x(t - d(t)) \\ f(x(t)) \\ f(x(t - d(t))) \end{bmatrix} \\ & + 2[x^T(t), x^T(t - d(t)), f^T(x(t)), f^T(x(t - d(t)))] \begin{bmatrix} X_{15} \\ X_{25} \\ X_{35} \\ X_{45} \end{bmatrix} (x(t) - x(t - d(t))) \\ & + \bar{d}\dot{x}^T(t) X_{55} \dot{x}(t) + x^T(t) F_1 x(t) - (1 - h)x^T(t - d(t)) F_1 x(t - d(t)) \\ & + f^T(x(t)) F_2 f(x(t)) - (1 - h)f^T(x(t - d(t))) F_2 f(x(t - d(t))) \\ & + 2[x^T(t) K N_1 f(x(t)) - f^T(x(t)) N_1 f(x(t))] \\ & + 2[x^T(t - d(t)) K N_2 f(x(t - d(t))) - f^T(x(t - d(t))) N_2 f(x(t - d(t)))] \\ & = [x^T(t), x^T(t - d(t)), f^T(x(t)), f^T(x(t - d(t)))] \Gamma \begin{bmatrix} x(t) \\ x(t - d(t)) \\ f(x(t)) \\ f(x(t - d(t))) \end{bmatrix}. \end{aligned} \tag{37}$$

□

According to condition (30), we arrive at the conclusion that $\dot{V}(t, x(t)) \leq 0$ ($V = 0$ only if $x = 0$); thus, the stationary solution $x = 0$ to system (7) is asymptotically stable. Next, when $h > 1$, we obtain a similar delay-dependent asymptotic stability criterion.

Proposition 5. *If $h > 1$ and there exist a symmetric positive definite matrix $P \in \mathbb{R}^{n \times n}$, and positive diagonal matrices $N_1 \in \mathbb{R}^{n \times n}$, $N_2 \in \mathbb{R}^{n \times n}$ such that the following LMIs hold:*

$$X = \begin{bmatrix} X_{11} & X_{12} & X_{13} & X_{14} & X_{15} \\ * & X_{22} & X_{23} & X_{24} & X_{25} \\ * & * & X_{33} & X_{34} & X_{35} \\ * & * & * & X_{44} & X_{45} \\ * & * & * & * & X_{55} \end{bmatrix} \geq 0, \tag{38}$$

$$\Gamma = \begin{bmatrix} \eta_{11} & \eta_{12} & \eta_{13} & \eta_{14} \\ * & \eta_{22} & \eta_{23} & \eta_{24} \\ * & * & \eta_{33} & \eta_{34} \\ * & * & * & \eta_{44} \end{bmatrix} < 0, \tag{39}$$

where

$$\begin{aligned} \eta_{11} &= -PI - IP + X_{15}^T + X_{15} + \bar{d}X_{55} + \bar{d}X_{11}, \\ \eta_{12} &= X_{25}^T - X_{15} + \bar{d}X_{12}, \\ \eta_{13} &= PW_0 + X_{35}^T + KN_1 - E^T - \bar{d}X_{55}W_0 + \bar{d}X_{13}, \\ \eta_{14} &= P\tilde{W} + X_{45}^T - \bar{d}X_{55}\tilde{W} + \bar{d}X_{14}, \\ \eta_{22} &= -X_{25}^T - X_{25} + \bar{d}X_{22}, \\ \eta_{23} &= -X_{35}^T + \bar{d}X_{23}, \\ \eta_{24} &= -X_{45}^T + KN_2 + \bar{d}X_{24}, \\ \eta_{33} &= -2N_1 + EW_0 + W_0^T E^T + \bar{d}W_0^T X_{55}W_0 + \bar{d}X_{33}, \\ \eta_{34} &= E\tilde{W} + \bar{d}W_0^T X_{55}\tilde{W} + \bar{d}X_{34}, \\ \eta_{44} &= -2N_2 + \bar{d}\tilde{W}^T X_{55}\tilde{W} + \bar{d}X_{44}, \end{aligned}$$

then, the stationary solution $x = 0$ to system (7) is asymptotically stable.

Proof of Proposition 5. Constructing the Lyapunov–Krasovskii functionals as follows:

$$V(t, x(t)) = V_1(t, x(t)) + V_2(t, x(t)) + V_3(t, x(t)) + V_4(t, x(t)), \tag{40}$$

where

$$\begin{aligned} V_1(t, x(t)) &= x^T(t)Px(t), \\ V_2(t, x(t)) &= 2 \sum_{i=1}^n e_i \int_0^{x_i(t)} f_i(y)dy, \\ V_3(t, x(t)) &= \int_0^t \int_{\delta-d(t)}^{\delta} v^T Xv dy d\delta, \\ V_4(t, x(t)) &= \int_{t-d}^t (\bar{d} + y - t) \dot{x}^T(y) X_{55} \dot{x}(y) dy. \end{aligned}$$

$e_i (i = 1, \dots, n)$ are positive scalars and $v = [x^T(\delta), x^T(\delta - d(\delta)), f^T(x(\delta)), f^T(x(\delta - d(\delta))), \dot{x}^T(y)]^T$, and combining (32)–(35), we have

$$\begin{aligned} \dot{V}(t, x(t)) &= \dot{V}_1(t, x(t)) + \dot{V}_2(t, x(t)) + \dot{V}_3(t, x(t)) + \dot{V}_4(t, x(t)) \\ &\leq [x^T(t), x^T(t - d(t)), f^T(x(t)), f^T(x(t - d(t)))] \Gamma \begin{bmatrix} x(t) \\ x(t - d(t)) \\ f(x(t)) \\ f(x(t - d(t))) \end{bmatrix}. \tag{41} \end{aligned}$$

□

According to condition (39), $\dot{V}(t, x(t)) \leq 0$ ($V = 0$ only if $x = 0$), which indicates that the stationary solution $x = 0$ to system (7) is asymptotically stable. Note that Propositions 3–5 are sufficient criteria for the asymptotic stability of system (7), where Proposition 3 is a delay-independent criterion and the others are delay-dependent criteria.

The particular states of neurons in insects’ navigation system are expressed and stabilized by the persistent activity of insects [46]. Considering the experimental observations [2,11,15,16,22], the asymptotic stability of the equilibrium point in the invariant set of system (7) may represent that the mechanisms of optimal cue integration have the ability to drive insects to robustly return to a unique target (nest). Based on the above propositions, it is precisely due to continuous external navigational cue inputs and the uniqueness and stability of the system’s equilibrium point that insects are able to self-correct their routes, target their nest, and reach it without disturbances from the external environment.

4. Illustrative Examples

In order to combine our theoretical analysis with the realistic cases, some numerical simulation examples for system (7) are expounded in this section. The time delay functions and activation function used below are based on references [47–49], which focus on neural network stability and synchronization. First, we give an example of system (7) with the time delay converging to 1.

Example 1. We consider the following four-neuron coupled system with time-varying delay $d(t) = \frac{e^t}{1+e^t}$ ($\bar{d} = 1, h = 0.25$), where the activation function is $g(x) = \tanh(x)$, and the matrices are

$$W_0 = \begin{bmatrix} 0.15 & 0.28 & 0 & 0 \\ 0.28 & 0.16 & 0 & 0 \\ 0 & 0 & 0.12 & 0.17 \\ 0 & 0 & 0.17 & 0.20 \end{bmatrix}, \tilde{W} = \begin{bmatrix} 0 & 0 & -0.04 & -0.05 \\ 0 & 0 & -0.01 & -0.02 \\ 0.03 & 0.07 & 0 & 0 \\ 0.02 & 0.05 & 0 & 0 \end{bmatrix}, K = \begin{bmatrix} 0.3 & 0 & 0 & 0 \\ 0 & 0.5 & 0 & 0 \\ 0 & 0 & 0.7 & 0 \\ 0 & 0 & 0 & 0.8 \end{bmatrix}.$$

System (7) is then written as

$$\begin{aligned} \dot{x}_1(t) &= -x_1(t) + 0.15 * \tanh(x_1(t)) + 0.28 * \tanh(x_2(t)), \\ &\quad - 0.04 * \tanh(x_3(t - d(t))) - 0.05 * \tanh(x_4(t - d(t))), \\ \dot{x}_2(t) &= -x_2(t) + 0.28 * \tanh(x_1(t)) + 0.16 * \tanh(x_2(t)), \\ &\quad - 0.01 * \tanh(x_3(t - d(t))) - 0.02 * \tanh(x_4(t - d(t))), \\ \dot{x}_3(t) &= -x_3(t) + 0.12 * \tanh(x_3(t)) + 0.17 * \tanh(x_4(t)) \\ &\quad + 0.03 * \tanh(x_1(t - d(t))) + 0.07 * \tanh(x_2(t - d(t))), \\ \dot{x}_4(t) &= -x_4(t) + 0.17 * \tanh(x_3(t)) + 0.20 * \tanh(x_4(t)) \\ &\quad + 0.02 * \tanh(x_1(t - d(t))) + 0.05 * \tanh(x_2(t - d(t))). \end{aligned} \tag{42}$$

We can obtain the following matrices and scalars:

$$R = \begin{bmatrix} 25.944 & 0 & 0 & 0 \\ 0 & 42.195 & 0 & 0 \\ 0 & 0 & 55.232 & 0 \\ 0 & 0 & 0 & 63.988 \end{bmatrix}, V = \begin{bmatrix} 30.915 & 0 & 0 & 0 \\ 0 & 28.268 & 0 & 0 \\ 0 & 0 & 25.675 & 0 \\ 0 & 0 & 0 & 23.434 \end{bmatrix},$$

$$F_1 = \begin{bmatrix} 21.865 & -0.144 & 0 & 0 \\ -0.144 & 21.803 & 0 & 0 \\ 0 & 0 & 22.141 & -0.306 \\ 0 & 0 & -0.306 & 22.043 \end{bmatrix}, F_2 = \begin{bmatrix} 16.480 & -2.962 & 0 & 0 \\ -2.962 & 16.641 & 0 & 0 \\ 0 & 0 & 17.135 & -2.514 \\ 0 & 0 & -2.514 & 16.186 \end{bmatrix},$$

$$N_1 = \begin{bmatrix} 20.547 & 0 & 0 & 0 \\ 0 & 21.018 & 0 & 0 \\ 0 & 0 & 20.869 & 0 \\ 0 & 0 & 0 & 21.556 \end{bmatrix}, N_2 = \begin{bmatrix} 6.969 & 0 & 0 & 0 \\ 0 & 6.520 & 0 & 0 \\ 0 & 0 & 5.872 & 0 \\ 0 & 0 & 0 & 5.819 \end{bmatrix},$$

$$P = \begin{bmatrix} 20.412 & -0.184 & 0 & 0 \\ -0.184 & 20.333 & 0 & 0 \\ 0 & 0 & 20.766 & -0.392 \\ 0 & 0 & -0.392 & 20.641 \end{bmatrix}, q = 0.43, \gamma = 1.20.$$

According to Propositions 1–3 and the above matrices and scalars, the stationary solution $x = 0$ to system (7) is unique and delay-independent and asymptotically stable in the invariant set. Figure 1 shows the trajectories of solutions $x(t)$ with different initial states, which asymptotically converge to 0, and it indicates that the system formed by the interaction of two integration neurons and two uniform inhibition neurons has a bounded invariant set, and there exists a unique equilibrium point that is asymptotically stable under certain conditions. Under continuous external stimuli inputs, the firing rates of neurons in the insects’ brain stay within a range and ultimately stabilize toward a unique equilibrium point. This phenomenon aligns with realistic experimental observations. Once insects lock in the target location (nest), the mechanisms of optimal cue integration in the insects’ navigation system play a vital role in driving insects to return to their nest, even in the presence of spatiotemporal changes and weak noises.

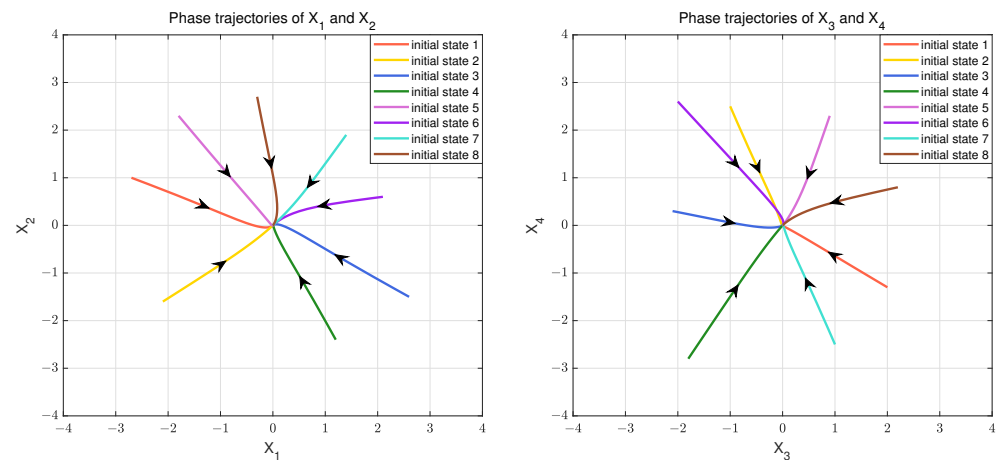


Figure 1. Phase trajectories of Example 1.

The above example shows the biological plausibility of system (7). We then give an example of system (7) with a time delay characterized by periodic oscillations with amplitudes in the range of 1 to illustrate the efficiency of other stability criteria

Example 2. We discuss the the following four-neuron coupled system with time-varying delay $d(t) = 0.8 - 0.1 * \sin(t)$ ($\bar{d} = 0.9, h = 0.1$), where the activation function is $g(x) = \tanh(x)$, and the matrices are

$$W_0 = \begin{bmatrix} 0.40 & 0.25 & 0 & 0 \\ 0.25 & 0.40 & 0 & 0 \\ 0 & 0 & 0.40 & 0.28 \\ 0 & 0 & 0.28 & 0.46 \end{bmatrix}, \tilde{W} = \begin{bmatrix} 0 & 0 & -0.01 & -0.05 \\ 0 & 0 & -0.02 & -0.01 \\ 0.13 & 0.16 & 0 & 0 \\ 0.10 & 0.15 & 0 & 0 \end{bmatrix}, K = \begin{bmatrix} 0.5 & 0 & 0 & 0 \\ 0 & 0.5 & 0 & 0 \\ 0 & 0 & 0.5 & 0 \\ 0 & 0 & 0 & 0.5 \end{bmatrix}.$$

Plugging in the above matrices, system (7) can take the form of (42). Thus, we have

$$R = \begin{bmatrix} 21.408 & 0 & 0 & 0 \\ 0 & 21.418 & 0 & 0 \\ 0 & 0 & 21.084 & 0 \\ 0 & 0 & 0 & 21.734 \end{bmatrix}, V = \begin{bmatrix} 33.330 & 0 & 0 & 0 \\ 0 & 33.338 & 0 & 0 \\ 0 & 0 & 33.102 & 0 \\ 0 & 0 & 0 & 32.654 \end{bmatrix},$$

$$F_1 = \begin{bmatrix} 14.480 & -0.216 & -0.015 & -0.001 \\ -0.216 & 14.481 & -0.015 & -0.012 \\ -0.015 & -0.015 & 14.401 & -0.313 \\ -0.001 & -0.012 & -0.313 & 14.330 \end{bmatrix}, F_2 = \begin{bmatrix} 9.440 & -2.040 & -0.003 & -0.003 \\ -2.040 & 9.460 & -0.003 & -0.003 \\ -0.003 & -0.003 & 9.432 & -2.277 \\ -0.003 & -0.003 & -2.277 & 9.114 \end{bmatrix},$$

$$N_1 = \begin{bmatrix} 20.365 & 0 & 0 & 0 \\ 0 & 20.380 & 0 & 0 \\ 0 & 0 & 20.137 & 0 \\ 0 & 0 & 0 & 20.545 \end{bmatrix}, N_2 = \begin{bmatrix} 10.063 & 0 & 0 & 0 \\ 0 & 10.120 & 0 & 0 \\ 0 & 0 & 9.990 & 0 \\ 0 & 0 & 0 & 10.089 \end{bmatrix},$$

$$P = \begin{bmatrix} 20.266 & -0.752 & -0.025 & -0.004 \\ -0.752 & 20.272 & -0.025 & -0.020 \\ -0.025 & -0.025 & 19.942 & -1.149 \\ -0.004 & -0.020 & -1.149 & 19.740 \end{bmatrix}, q = 0.89, \gamma = 0.76.$$

Clearly, it follows from Propositions 1, 2 and 4 that the unique stationary solution $x = 0$ to system (7) is delay-dependent and asymptotically stable (Figure 2). Compared with the delay-independent stability condition, the delay-dependent stability condition allows a finite time delay. In real bio-systems, the time delay is limited. The delay-dependent stability result takes the time delay into account and proposes an accurate condition that the system will be asymptotically stable within the upper bound of the time delay. Therefore, we suggest that the delay-dependent criterion is more accurate and has higher compatibility for systems with different time delay upper bound sizes. This criterion is superior to the delay-independent one, which helps to further explore the stability of the bounded time delay system in insects' brains.

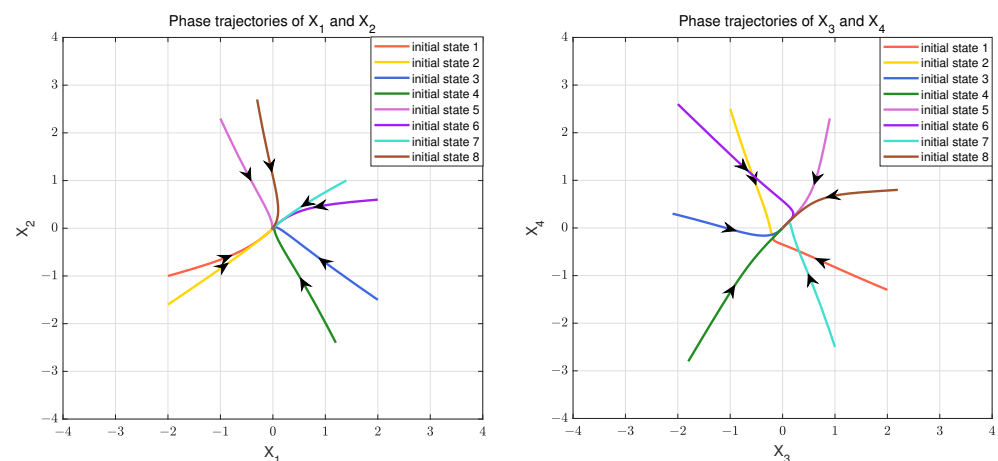


Figure 2. Phase trajectories of Example 2.

Finally, we give an example of system (7) with a time delay, the time delay being characterized by volatile slopes and a large upper bound.

Example 3. We consider the four-neuron coupled system with time-varying delay $d(t) = 2 + 2 * \sin(t)$ ($\bar{d} = 4, h = 2$), where the activation function is $g(x) = \tanh(x)$, and the matrices are

$$W_0 = \begin{bmatrix} 0.10 & 0.15 & 0 & 0 \\ 0.15 & 0.20 & 0 & 0 \\ 0 & 0 & 0.32 & 0.25 \\ 0 & 0 & 0.25 & 0.30 \end{bmatrix}, \tilde{W} = \begin{bmatrix} 0 & 0 & -0.21 & -0.16 \\ 0 & 0 & -0.20 & -0.14 \\ 0.20 & 0.23 & 0 & 0 \\ 0.25 & 0.22 & 0 & 0 \end{bmatrix}, K = \begin{bmatrix} 0.2 & 0 & 0 & 0 \\ 0 & 0.3 & 0 & 0 \\ 0 & 0 & 0.5 & 0 \\ 0 & 0 & 0 & 0.6 \end{bmatrix}.$$

Plugging in the matrices above, and system (7) will be in the form of (42). Then, we can obtain the following matrices and scalars:

$$R = \begin{bmatrix} 13.237 & 0 & 0 & 0 \\ 0 & 20.206 & 0 & 0 \\ 0 & 0 & 33.097 & 0 \\ 0 & 0 & 0 & 37.731 \end{bmatrix}, V = \begin{bmatrix} 28.904 & 0 & 0 & 0 \\ 0 & 27.735 & 0 & 0 \\ 0 & 0 & 23.700 & 0 \\ 0 & 0 & 0 & 21.759 \end{bmatrix},$$

$$N_1 = \begin{bmatrix} 54.017 & 0 & 0 & 0 \\ 0 & 56.846 & 0 & 0 \\ 0 & 0 & 68.658 & 0 \\ 0 & 0 & 0 & 66.939 \end{bmatrix}, N_2 = \begin{bmatrix} 52.316 & 0 & 0 & 0 \\ 0 & 46.212 & 0 & 0 \\ 0 & 0 & 27.576 & 0 \\ 0 & 0 & 0 & 20.856 \end{bmatrix},$$

$$P = \begin{bmatrix} 96.308 & -11.745 & 0.993 & 0.925 \\ -11.745 & 103.314 & 0.654 & 1.092 \\ 0.993 & 0.654 & 108.333 & -13.717 \\ 0.925 & 1.092 & -13.717 & 109.864 \end{bmatrix}, q = 0.59, \gamma = 1.40.$$

Under Propositions 1, 2 and 5, the stationary solution $x = 0$ to system (7) is unique and delay-dependent and asymptotically stable. Figure 3 shows phase trajectories of Example 3, and it indicates that the stationary solution $x = 0$ to this system is unique and asymptotically stable. This criterion helps to address the stability problem that the slope of time delay has large changes applied to situations where the communication between neurons has a long time delay.

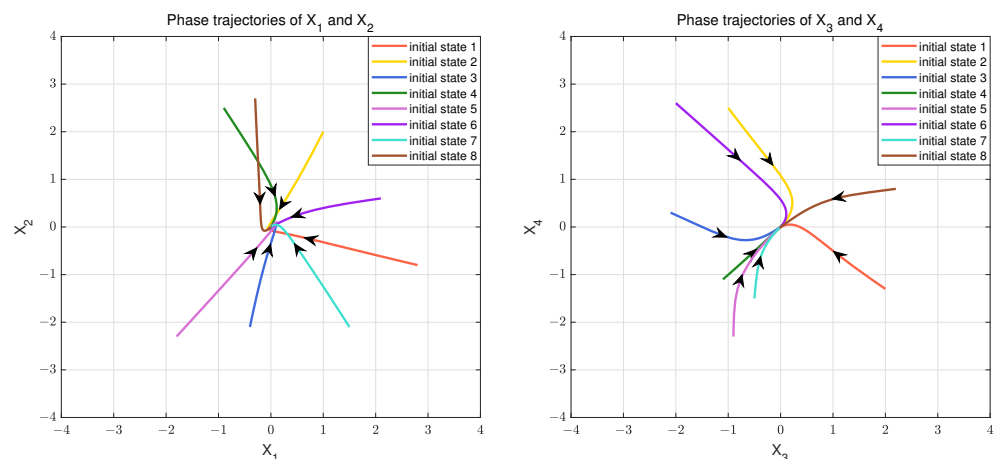


Figure 3. Phase trajectories of Example 3.

5. Conclusions

In this paper, we discuss the dynamical properties of optimal cue integration in the insects' navigation system. The system for optimal cue integration is considered a primary part of the navigational system, which coordinates different navigational strategies to guide insects directly to their nest. From a dynamical perspective and based on LMIs and

Lyapunov–Krasovskii functionals, we obtain that an invariant set exists in the system of optimal cue integration. Then, conditions for the uniqueness and stability of the equilibrium point are presented in this invariant set. Some experiments have confirmed that in the presence of light and odor cues, firing rates of neurons in insects' and mammals' brains are correlated with path integration and homing behaviors. Therefore, the obtained conditions may effectively demonstrate the neural mechanisms of the system of optimal cue integration, which drive insects to successfully return to their nests under environmental noises. This provides a theoretical basis for the research of insect-inspired AI and promotes further investigation of the autonomous, mobile robots with high computing capability and parsimony. In the future, we will focus on the multistability of the insects' navigation systems.

Author Contributions: Conceptualization, M.L.; methodology, M.L., D.L. and J.Z.; software, M.L. and D.L.; formal analysis, M.L.; investigation, M.L. and D.Z.; visualization, M.L. and J.Z.; writing—original draft, M.L.; writing—review & editing M.L., D.L., J.Z. and X.X.; validation, M.L. and X.X. All authors have read and agreed to the published version of the manuscript.

Funding: This work was supported in part by the Natural Science Foundation of Guangxi under Grant 2022GXNSFAA035519.

Data Availability Statement: Data will be made available on request.

Conflicts of Interest: The authors declare no conflict of interest.

References

1. Webb, B.; Wystrach, A. Neural mechanisms of insect navigation. *Curr. Opin. Insect Sci.* **2016**, *15*, 27–39. [[CrossRef](#)]
2. Hulse, B.; Haberkern, H.; Franconville, R.; Turner-Evans, D.; Takemura, S.; Wolff, T.; Noorman, M.; Dreher, M.; Dan, C.; Parekh, R.; et al. A connectome of the *Drosophila* central complex reveals network motifs suitable for flexible navigation and context-dependent action selection. *eLife* **2021**, *10*, e66039. [[CrossRef](#)] [[PubMed](#)]
3. Ko, H.; Hofer, S.B.; Pichler, B.; Buchanan, K.A.; Sjoestroem, P.J.; Mrcic-Flogel, T.D. Functional Specificity of Local Synaptic Connections in Neocortical Networks. *Nature* **2011**, *473*, 87. [[CrossRef](#)]
4. Mysore, S.P.; Asadollahi, A.; Knudsen, E.I. Global Inhibition and Stimulus Competition in the Owl Optic Tectum. *J. Neurosci. Off. J. Soc. Neurosci.* **2010**, *30*, 1727–1738. [[CrossRef](#)] [[PubMed](#)]
5. Ozeki, H.; Finn, I.M.; Schaffer, E.S.; Miller, K.D.; Ferster, D. Inhibitory Stabilization of the Cortical Network Underlies Visual Surround Suppression. *Neuron* **2009**, *62*, 578–592. [[CrossRef](#)] [[PubMed](#)]
6. Weliky, M.; Kandler, K.; Fitzpatrick, D.; Katz, L.C. Patterns of Excitation and Inhibition Evoked by Horizontal Connections in Visual Cortex Share a Common Relationship to Orientation Columns. *Neuron* **1995**, *15*, 541–552. [[CrossRef](#)]
7. Wu, S.; Hamaguchi, K.; Amari, S. Dynamics and Computation of Continuous Attractors. *Neural Comput.* **2008**, *20*, 994–1025. [[CrossRef](#)]
8. You, H.; Zhao, K. Neuromorphic Implementation of a Continuous Attractor Neural Network With Various Synaptic Dynamics. *IEEE Access* **2021**, *9*, 109224–109240. [[CrossRef](#)]
9. Khona, M.; Fiete, I.R. Attractor and integrator networks in the brain. *Nat. Rev. Neurosci.* **2022**, *23*, 744–766. [[CrossRef](#)]
10. Zhang, W.; Wu, Y.N.; Wu, S. Translation-equivariant Representation in Recurrent Networks with a Continuous Manifold of Attractors. In Proceedings of the Neural Information Processing Systems, New Orleans, LA, USA, 28 November–9 December 2022; Volume 35, pp. 15770–15783.
11. Kim, S.S.; Rouault, H.; Druckmann, S.; Jayaraman, V. Ring attractor dynamics in the *Drosophila* central brain. *Science* **2017**, *356*, 849–853. [[CrossRef](#)]
12. Zhang, W.; Wang, H.; Chen, A.; Gu, Y.; Lee, T.; Wong, K.M.; Wu, S. Complementary Congruent and Opposite Neurons Achieve Concurrent Multisensory Integration and Segregation. *eLife* **2019**, *8*, e43753. [[CrossRef](#)]
13. Okubo, T.S.; Patella, P.; D'Alessandro, I.; Wilson, R.I. A Neural Network for Wind-Guided Compass Navigation. *Neuron* **2020**, *107*, 924–940.e18. [[CrossRef](#)]
14. Jung, S.H.; Hueston, C.; Bhandawat, V. Odor-identity dependent motor programs underlie behavioral responses to odors. *eLife* **2015**, *4*, e11092. [[CrossRef](#)]
15. Sun, X.; Yue, S.; Mangan, M. A Decentralised Neural Model Explaining Optimal Integration of Navigational strategies in insects. *eLife* **2020**, *9*, e54026. [[CrossRef](#)] [[PubMed](#)]
16. Sun, X.; Yue, S.; Mangan, M. How the Insect Central Complex could Coordinate Multimodal Navigation. *eLife* **2021**, *10*, e73077. [[CrossRef](#)]
17. de Croon, G.C.H.E.; Dupeyroux, J.J.G.; Fuller, S.B.; Marshall, J.A.R. Insect-inspired AI for autonomous robots. *Sci. Robot.* **2022**, *7*, eabl6334. [[CrossRef](#)] [[PubMed](#)]

18. Petrucco, L.; Lavian, H.; Wu, Y.K.; Svara, F.; Štih, V.; Portugues, R. Neural dynamics and architecture of the heading direction circuit in zebrafish. *Nat. Neurosci.* **2023**, *26*, 765–773. [[CrossRef](#)]
19. Foster, D.J.; Knierim, J.J. Sequence learning and the role of the hippocampus in rodent navigation. *Curr. Opin. Neurobiol.* **2012**, *22*, 294–300. [[CrossRef](#)] [[PubMed](#)]
20. Sun, X.; Mangan, M.; Yue, S. An Analysis of a Ring Attractor Model for Cue Integration. *Biomim. Biohybrid Syst.* **2018**, *10928*, 459–470.
21. Qin, S.; Farashahi, S.; Lipshutz, D.; Sengupta, A.M.; Chklovskii, D.B.; Pehlevan, C. Coordinated drift of receptive fields in Hebbian/anti-Hebbian network models during noisy representation learning. *Nat. Neurosci.* **2023**, *26*, 339–349. [[CrossRef](#)] [[PubMed](#)]
22. Vedder, L.C.; Miller, A.M.; Harrison, M.B.; Smith, D.M. Retrosplenial Cortical Neurons Encode Navigational Cues, Trajectories and Reward Locations during Goal Directed Navigation. *Cereb. Cortex* **2017**, *27*, 3713–3723. [[CrossRef](#)]
23. Wilson, R.I. Neural Networks for Navigation: From Connections to Computations. *Annu. Rev. Neurosci.* **2023**, *46*, 403–423. [[CrossRef](#)] [[PubMed](#)]
24. Vafidis, P.; Oswald, D.; D’Albis, T.; Kempter, R. Learning accurate path integration in ring attractor models of the head direction system. *eLife* **2022**, *11*, e69841. [[CrossRef](#)] [[PubMed](#)]
25. Kutschireiter, A.; Basnak, M.A.; Wilson, R.I.; Drugowitsch, J. Bayesian inference in ring attractor networks. *Proc. Natl. Acad. Sci. USA* **2023**, *120*, e2210622120. [[CrossRef](#)]
26. Yu, J.; Chen, W.; Leng, J.; Wang, C.; Yi, Z. Weight Matrix as a Switch Between Line Attractor and Plane Attractor of Ring Neural Networks. *Neurocomputing* **2023**, *521*, 181–188. [[CrossRef](#)]
27. Hoinville, T.; Wehner, R. Optimal multiguideance integration in insect navigation. *Proc. Natl. Acad. Sci. USA* **2018**, *115*, 2824–2829. [[CrossRef](#)] [[PubMed](#)]
28. Wang, Y.; Zhu, S.; Shao, H.; Feng, Y.; Wang, L.; Wen, S. Comprehensive analysis of fixed-time stability and energy cost for delay neural networks. *Neural Netw.* **2022**, *155*, 413–421. [[CrossRef](#)]
29. Udhayakumar, K.; Rihan, F.A.; Rakkiyappan, R.; Cao, J. Fractional-Order Discontinuous Systems with Indefinite LKFs: An Application to Fractional-Order Neural Networks with Time Delays. *Neural Netw.* **2021**, *145*, 319–330. [[CrossRef](#)]
30. Wang, X.; Cao, J.; Wang, J.; Qi, J.; Sun, Q. A Novel Fast Fixed-Time Control Strategy and Its Application to Fixed-Time Synchronization Control of Delayed Neural Networks. *Neural Process. Lett.* **2021**, *54*, 145–164. [[CrossRef](#)]
31. Hu, Y.; Hu, G. Stabilization and Chaos Control of an Economic Model via a Time-Delayed Feedback Scheme. *Mathematics* **2023**, *11*, 2994. [[CrossRef](#)]
32. Rahman, B.; Blyuss, K.B.; Kyrychko, Y.N. Dynamics of Neural Systems with Discrete and Distributed Time Delays. *SIAM J. Appl. Dyn. Syst.* **2015**, *14*, 2069–2095. [[CrossRef](#)]
33. Erneux, T.; Javaloyes, J.; Wolfrum, M.; Yanchuk, S. Introduction to Focus Issue: Time-delay dynamics. *Chaos Interdiscip. J. Nonlinear Sci.* **2017**, *27*, 114201. [[CrossRef](#)] [[PubMed](#)]
34. Protachevich, P.R.; Borges, F.S.; Iarosz, K.C.; Baptista, M.S.; Lameu, E.L.; Hansen, M.; Caldas, I.L.; Szezech, J.D.; Batista, A.M.; Kurths, J. Influence of Delayed Conductance on Neuronal Synchronization. *Front. Physiol.* **2020**, *11*, 1053–1062. [[CrossRef](#)] [[PubMed](#)]
35. Guo, M.; Zhu, S.; Liu, X. Observer-Based State Estimation for Memristive Neural Networks with Time-Varying Delay. *Knowl.-Based Syst.* **2022**, *246*, 108707. [[CrossRef](#)]
36. Zheng, W.; Lam, H.K.; Sun, F.; Wen, S. Robust Stability Analysis and Feedback Control for Uncertain Systems With Time-Delay and External Disturbance. *IEEE Trans. Fuzzy Syst.* **2022**, *30*, 5065–5077. [[CrossRef](#)]
37. Maharajan, C.; Raja, R.; Cao, J.; Rajchakit, G.; Alsaedi, A. Impulsive Cohen–Grossberg BAM Neural Networks with Mixed Time-Delays: An Exponential Stability Analysis Issue. *Neurocomputing* **2018**, *275*, 2588–2602. [[CrossRef](#)]
38. Chen, X.; Liu, Y.; Ruan, Q.; Cao, J. Stabilization of Nonlinear Time-Delay Systems: Flexible Delayed Impulsive Control. *Appl. Math. Model.* **2023**, *114*, 488–501. [[CrossRef](#)]
39. Zhou, L. Global Asymptotic Stability of Cellular Neural Networks with Proportional Delays. *Nonlinear Dyn.* **2014**, *77*, 41–47. [[CrossRef](#)]
40. Hua, C.; Long, C.; Guan, X. New Results on Stability Analysis of Neural Networks with Time-Varying Delays. *Phys. Lett. A* **2006**, *352*, 335–340. [[CrossRef](#)]
41. Moon, Y.S.; Park, P.; Kwon, W.H.; Lee, Y.S. Delay-dependent robust stabilization of uncertain state-delayed systems. *Int. J. Control* **2001**, *74*, 1447–1455. [[CrossRef](#)]
42. Zeng, H.; Zhou, S.; Zhang, X.; Wang, W. Delay-Dependent Stability Analysis of Load Frequency Control Systems With Electric Vehicles. *IEEE Trans. Cybern.* **2022**, *52*, 13645–13653. [[CrossRef](#)] [[PubMed](#)]
43. Wang, X.; Park, J.H.; Yang, H.; Zhong, S. Delay-Dependent Stability Analysis for Switched Stochastic Networks With Proportional Delay. *IEEE Trans. Cybern.* **2022**, *52*, 6369–6378. [[CrossRef](#)] [[PubMed](#)]
44. Mao, X.; Sun, J.Q.; Li, S. Dynamics of delay-coupled FitzHugh–Nagumo neural rings. *Chaos Interdiscip. J. Nonlinear Sci.* **2018**, *28*, 013104. [[CrossRef](#)] [[PubMed](#)]
45. Shao, H.; Li, H.; Shao, L. Improved delay-dependent stability result for neural networks with time-varying delays. *ISA Trans.* **2018**, *80*, 1000–1005. [[CrossRef](#)]

46. Hopfield, J.J. Neurons with graded response have collective computational properties like those of two-state neurons. *Proc. Natl. Acad. Sci. USA* **1984**, *81*, 3088–3092. [[CrossRef](#)]
47. Sharma, S.; Sharma, S.; Athaiya, A. Activation functions in neural networks. *Towards Data Sci.* **2017**, *6*, 310–316. [[CrossRef](#)]
48. Sheng, Y.; Zeng, Z.; Huang, T. Finite-Time Stabilization of Competitive Neural Networks With Time-Varying Delays. *IEEE Trans. Cybern.* **2022**, *52*, 11325–11334. [[CrossRef](#)]
49. Zheng, C.; Hu, C.; Yu, J.; Jiang, H. Fixed-time synchronization of discontinuous competitive neural networks with time-varying delays. *Neural Netw.* **2022**, *153*, 192–203. [[CrossRef](#)]

Disclaimer/Publisher’s Note: The statements, opinions and data contained in all publications are solely those of the individual author(s) and contributor(s) and not of MDPI and/or the editor(s). MDPI and/or the editor(s) disclaim responsibility for any injury to people or property resulting from any ideas, methods, instructions or products referred to in the content.